

## THE APPLICATION OF COMPUTER ALGEBRA IN MODELLING AND VIBRATION CONTROL OF A FLEXIBLE MANIPULATOR

Z. MOHAMED<sup>1</sup>, A. A. MOHD FAUDZI<sup>2</sup>, M. N. AHMAD<sup>3</sup>, Z. M. ZAIN<sup>4</sup>  
& A. W. I. MOHD HASHIM<sup>5</sup>

**Abstract.** This paper presents the application of computer algebra to modelling and vibration control of a flexible manipulator system. A symbolic-based model characterising the behaviour of the manipulator is developed using a symbolic language based on finite element and Lagrange methods. In this approach, the system transfer function is obtained in symbolic form. Analyses are carried out to investigate the significance and relations of the physical parameters of the flexible manipulator with the system characteristics including poles, zeros, stability, vibration frequencies and non-minimum phase characteristics of the system. The symbolic results are then used to design an effective input shaping vibration control scheme. Simulation results of the response of the manipulator are presented to demonstrate the application of the symbolic algorithm in modelling and control of a flexible manipulator. The symbolic results are then used to design an effective input shaping vibration control scheme. Simulation results of the response of the manipulator are presented to demonstrate the application of the symbolic algorithm in modelling and control of a flexible manipulator.

**Keywords:** Computer algebra; flexible manipulator; modelling; vibration control

**Abstrak.** Kertas kerja ini membentangkan aplikasi algebra computer utk pemodelan dan kawalan getaran sistem *manipulator* boleh ubah (*flexible manipulator*). Sebuah model berasaskan simbol menspesifikasikan sifat *manipulator* telah dibina menggunakan bahasa simbolik berasaskan *finite element* dan *Lagrange*. Menggunakan pendekatan ini, *transfer function* diperolehi dalam bentuk simbolik. Analisis dilaksanakan untuk mengkaji signifikan dan relasi pemboleh ubah fizikal *manipulator* boleh ubah tersebut dengan sistem tertentu termasuk *poles*, *zeros*, kestabilan, frekuensi getaran dan tertentu fasa *non minimum* sistem tersebut. Hasil akhir simbolik tersebut kemudian digunakan untuk mereka cipta *input shaping* getaran skema kawalan. Hasil akhir simulasi dari respons manipulator dibentangkan untuk mendemonstrasi aplikasi algorithm dalam pemodelan dan kawalan sesebuah *manipulator* boleh ubah.

**Kata kunci:** Algebra computer, *manipulator* boleh ubah, pemodelan, kawalan getaran

---

<sup>1-5</sup> Faculty of Electrical Engineering, Universiti Teknologi Malaysia, 81310 UTM Johor Bahru, Johor Darul Ta'azim

## 1.0 INTRODUCTION

Flexible robot manipulators exhibit several advantages over rigid robots. They are lighter in weight, consume less power, require smaller actuators, are more manoeuvrable and transportable, have less overall cost and higher payload to robot weight ratio. Due to such advantages, flexible robot manipulators are used in various applications including space exploration and hazardous environments. However, control of flexible manipulators to maintain accurate positioning is a challenging problem. Problems arise due to precise positioning requirement, vibration due to system flexibility and the difficulty in obtaining accurate model for the system. The complexity of this problem increases dramatically when a flexible manipulator carries a payload. Previous investigations have shown that the dynamic behaviour of the manipulator is significantly affected by payload variations [1]. If the advantages associated with lightness are not to be sacrificed, accurate models and efficient controllers have to be developed.

Various approaches have previously been developed for modelling of flexible manipulators. These include assumed modes method, finite difference and finite element (FE) methods to solve the partial differential equation characterising the dynamic behaviour of a flexible manipulator system. Previous simulation and experimental investigations on two flexible manipulator systems have shown that the methods can be utilised to obtain a good representation of the actual systems [2]. Moreover, using the FE method, a single element is sufficient to describe the dynamic behaviour of a flexible manipulator reasonably well [3]. However, most of the developments are numerical-based. Dynamic characteristics of the manipulator both in time and frequency domains are investigated on the basis of a single particular case, with no provision for any generality [3]. Moreover, numerical systems must operate using numeric approximations, whose precision is limited by the computer hardware. Alternatively, exact quantities can be obtained by retaining the computations in a symbolic form using computer algebra. A distinguishing feature of symbolic-based methods is the mathematically comprehensive output they generate, so that the significance of individual terms, or group of terms, may be identified. Whenever possible, closed-form solutions are obtained. This brings with it the opportunity to gain insights into the model that would otherwise not be available. Computer algebra will open up the possibility of analysing a flexible manipulator system in an effective way [4].

Symbolic algebra for modelling and simulation of flexible manipulators has previously been investigated. Most of these investigations have developed automated symbolic derivations of dynamic equations of motion of rigid and flexible manipulators utilising Lagrangian formulation and assumed mode methods [5, 6]. In [5], a symbolic dynamic model for robotic manipulators with flexible link is obtained by writing the system lagrangian and then using the Euler-

Lagrange equation to obtain the model. This process can be automated as evidenced by the REDUCE script. In [7], an infinite-dimensional model is developed using symbolic manipulation. From this model, the effect of link parameters and different boundary conditions can be explicitly seen. Alternative approaches to symbolic modelling include the use of Hamilton's principle and non-linear integro-differential equations [8] and finite difference approximations [9]. These have demonstrated that the approach has some advantages, such as allowing independent variation of flexure parameters. On the other hand, not much work has been reported on the application of symbolic algebra for control of flexible manipulators.

This paper presents the application of computer algebra to modelling and vibration control of a flexible robot manipulator system. Although, computer algebra has been utilised for modelling of the system, not much work has been done on the development of controllers. A constrained planar single-link flexible robot manipulator is considered. As the FE method has been demonstrated to provide a satisfactory dynamic model of the system, it is desirable to derive a symbolic-based model based on the method. In this work, Macsyma, a language based on computer algebra is utilised for development of an automated symbolic derivation of the dynamic model of the system using the FE and Lagrange methods with different number of elements. Using computer algebra, an error-free and good approximation of the transfer function representing the actual flexible manipulator in terms of system parameters such as length, weight, flexural rigidity and payload is obtained. Analyses are then carried out to investigate the significance and relations of the physical parameters of the flexible manipulator with the system characteristics including poles, zeros, stability, vibration frequencies and non-minimum phase characteristics. In particular, the effects of payload on the manipulator is important for modelling and control purposes, as successful implementation of a flexible manipulator control is contingent upon achieving acceptable uniform performance in the presence of payload variations. In control, an input shaping control is developed based on symbolic algebra to suppress the vibration of the system with varying payloads. As payload changes, the input shaper can be updated automatically using closed form equations derived from symbolic algebra to achieve a similar level of vibration reduction. Simulation results of the response of the manipulator are presented to demonstrate the application of the symbolic algorithm in control of a flexible manipulator. Finally, several advantages of using computer algebra for modelling and vibration control of flexible manipulators are highlighted and discussed.

### 1.0 THE FLEXIBLE MANIPULATOR SYSTEM

A mechanical model of the single-link flexible manipulator system considered in this work is shown in Fig. 1, where  $X_oOY_o$  and  $XOY$  represent the stationary and moving co-ordinate frames respectively. The axis  $OX$  coincides with the neutral line of the link in its undeformed configuration, and is tangent to it at the clamped end in a deformed configuration.  $\tau$  represents the applied torque at the hub.  $E$ ,  $L$ ,  $I$ ,  $\rho$ ,  $A$ ,  $I_h$  and  $M_p$  represent the Young modulus, length, area moment of inertia, mass density per unit volume, cross sectional area, hub inertia and payload of the manipulator respectively.  $\theta(t)$  denotes an angular displacement (hub-angle) of the manipulator and  $w(x,t)$  denotes an elastic deflection of a point along the manipulator at a distance  $x$  from the hub of the manipulator. In this work, the motion of the manipulator is confined to the  $X_oOY_o$  plane. The manipulator is assumed to be stiff in vertical bending and torsion, allowing it to vibrate dominantly in the horizontal direction and thus, the gravity effects are neglected. Moreover, the manipulator is considered to have constant cross section and uniform material properties throughout

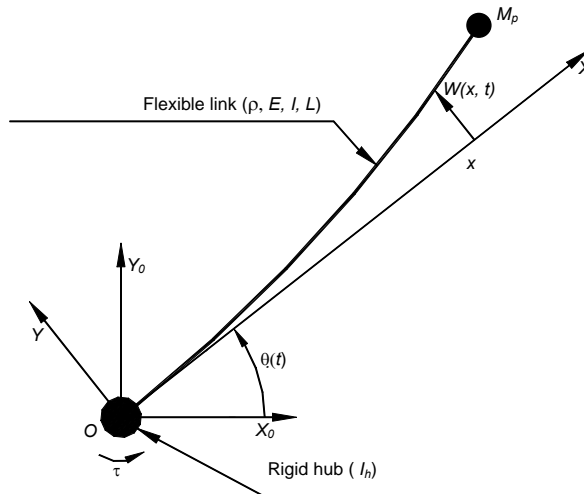


**Figure 1** Mechanical model of the flexible manipulator system.

### 3.0 SYMBOLIC-BASED MODEL DEVELOPMENT

This section focuses on the development of the symbolic-based model in characterising the dynamic behaviour of the flexible manipulator system. The dynamic equations of motion of the system are derived using the FE and Lagrange methods. A flow chart of the overall modelling approach for the general case of  $n$  elements is shown in Figure 2. In this approach, all the manipulations are carried out symbolically using Macsyma. The overall approach involves treating the flexible manipulator as an assemblage of  $n$  elements of length  $l$ . For each of these elements, mass and stiffness matrices are computed based on kinetic and potential energies of the system. The matrices are then assembled to form system mass and stiffness matrices. Subsequently, the Lagrange equation is utilised to obtain the dynamic equation of motion of the flexible manipulator. In this work, a transfer function from torque input to end-point residual output of the manipulator is considered. The modelling approach utilised in this work has previously been developed based on numerical simulation and has been validated with experimental exercises [2].

#### 3.1 Dynamic Equation of Motion

Another consideration also should be taken into account is about the feedback signal from the sensor jig itself. As mention above aluminium and PVC are two types of material that are used for the sensor jig. Figure 7 shows the different value of adjacent voltage when using different material of sensor jig.

The total displacement  $y(x, t)$  of a point along the manipulator at a distance  $x$  from the hub can be obtained as

$$y(x, t) = x\theta(t) + w(x, t) \quad (1)$$

Using the FE method to solve dynamic problems leads to the well-known equation

$$w(x, t) = N_a(x) Q_a(t) \quad (2)$$

where  $N_a(x)$  and  $Q_a(t)$  represent the shape function and nodal displacement respectively. Hence, the displacement can be obtained as

$$y(x, t) = N(x) Q(t) \quad (3)$$

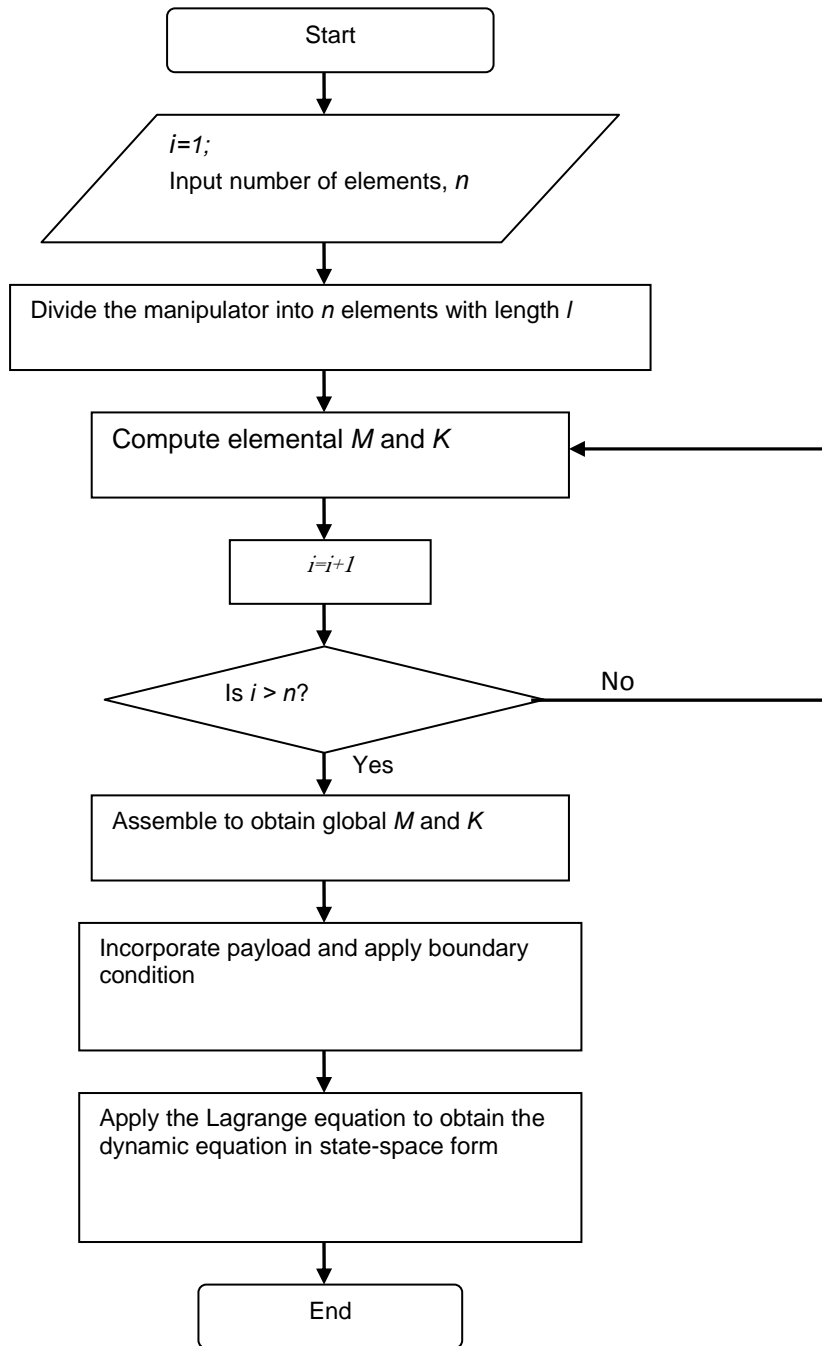


**Figure 2** Flow chart of the symbolic model development approach

where

$$N(x) = [x \quad N_a(x)] \text{ and } Q(t) = [\theta(t) \quad Q_a(t)]^T$$

The shape function  $N(x)$  and nodal displacement vector  $Q(t)$  in Eq. (3) incorporate local and global variables. Among these, the angle  $\theta(t)$  and the distance  $x$  are global variables while  $N_a(x)$  and  $Q_a(t)$  are local variables.

Defining  $k = x - \sum_{i=1}^{n-1} l_i$  as a local variable of the  $n$ th element, where  $l_i$  is the length of the  $i$ th element and utilising Macsyma, the shape function can be expressed in symbolic form as

$$N(k) = \left[ k + l(n-1) \quad 1 - \frac{3k^2}{l^2} + \frac{2k^3}{l^3} \quad k - \frac{2k^2}{l} + \frac{k^3}{l^2} \quad \frac{3k^2}{l^2} - \frac{2k^3}{l^3} \quad -\frac{k^2}{l} + \frac{k^3}{l^2} \right] \tag{4}$$

Defining

$$M_n = \int_0^l \rho A(N^T N) dk = \text{element mass matrix} \tag{5}$$

$$K_n = \int_0^l EI(\Phi^T \Phi) dk = \text{element stiffness matrix} \tag{6}$$

where  $\Phi = \frac{d^2 N(k)}{dk^2} = \left[ 0 \quad \frac{12k}{l^3} - \frac{6}{l^2} \quad \frac{6k}{l^2} - \frac{4}{l} \quad \frac{6}{l^2} - \frac{12k}{l^3} \quad \frac{6k}{l^2} - \frac{2}{l} \right]$  and solving Eqs. (5) and (6) for  $n$  elements, the elemental mass and stiffness matrices can be obtained as

$$M_n = \frac{\rho Al}{420} \begin{bmatrix} 140l^2(3n^2 - 3n + 1) & 21l(10n - 7) & 7l^2(5n - 3) & 21l(10n - 3) & -7l^2(5n - 2) \\ 21l(10n - 7) & 156 & 22l & 54 & -13l \\ 7l^2(5n - 3) & 22l & 4l^2 & 13l & -3l^2 \\ 21l(10n - 3) & 54 & 13l & 156 & -22l \\ -7l^2(5n - 2) & -13l & -3l^2 & -22l & 4l^2 \end{bmatrix}$$

$$K_n = \frac{EI}{l^3} \begin{bmatrix} 0 & 0 & 0 & 0 & 0 \\ 0 & 12 & 6l & -12 & 6l \\ 0 & 6l & 4l^2 & -6l & 2l^2 \\ 0 & -12 & -6l & 12 & -6l \\ 0 & 6l & 2l^2 & -6l & 4l^2 \end{bmatrix} \tag{7}$$

The matrices from above are assembled to obtain mass and stiffness matrices of the system,  $M$  and  $K$ , and used in the Lagrange equation to obtain the dynamic equation of the flexible manipulator as

$$M\ddot{Q}(t) + KQ(t) = F(t) \tag{8}$$

where  $F(t)$  is the vector of torques and  $Q(t) = [\theta \ w_0 \ \theta_0 \ \dots \ w_\alpha \ \theta_\alpha]^T$ .  $w_\alpha$  and  $\theta_\alpha$  are end-point residual and rotation of the manipulator respectively. Using a single element,  $n = 1$ , the dynamic equation of motion of the flexible manipulator can be obtained as in Eq. (8) with

$$M = \frac{\rho Al}{420} \begin{bmatrix} 140l^2 & 63l & 14l^2 & 147l & -21l^2 \\ 63l & 156 & 22l & 54 & -13l \\ 14l^2 & 22l & 4l^2 & 13l & -3l^2 \\ 147l & 54 & 13l & 156 & -22l \\ -21l^2 & -13l & -3l^2 & -22l & 4l^2 \end{bmatrix}, \tag{9}$$

$$K = \frac{EI}{l^3} \begin{bmatrix} 0 & 0 & 0 & 0 & 0 \\ 0 & 12 & 6l & -12 & 6l \\ 0 & 6l & 4l^2 & -6l & 2l^2 \\ 0 & -12 & -6l & 12 & -6l \\ 0 & 6l & 2l^2 & -6l & 4l^2 \end{bmatrix},$$

$$Q(t) = [\theta \ w_0 \ \theta_0 \ w_\alpha \ \theta_\alpha]^T \text{ and } F(t) = [\tau \ 0 \ 0 \ 0 \ 0]^T.$$

By incorporating the payload, hub inertia and initial conditions into the dynamic model of the system, a new dynamic equation of motion can be obtained as



$$M = \frac{\rho Al}{420} \begin{bmatrix} 140l^2 + l^2 M_p + I_h & 147l + l M_p & -21l^2 \\ 147l + l M_p & 156 + M_p & -22l \\ -21l^2 & -22l & 4l^2 \end{bmatrix} \quad K = \frac{EI}{l^3} \begin{bmatrix} 0 & 0 & 0 \\ 0 & 12 & -6l \\ 0 & -6l & 4l^2 \end{bmatrix}, \quad (10)$$

$$Q(t) = [\theta \quad w_\alpha \quad \theta_\alpha]^T \quad \text{and} \quad F(t) = [\tau \quad 0 \quad 0]^T.$$

For control purposes, the matrix differential equation in Eq. (8) is represented in a state-space form as

$$\begin{aligned} \dot{v} &= Av + Bu \\ y &= Cv \end{aligned} \quad (11)$$

where

$$A = \left[ \begin{array}{c|c} \mathbf{0}_3 & I_3 \\ \hline -M^{-1}K & \mathbf{0}_3 \end{array} \right], \quad B = \left[ \begin{array}{c} \mathbf{0}_{3 \times 1} \\ M_1^{-1} \end{array} \right]$$

$u = [\tau]$  and the state,  $v = [\theta \quad w_\alpha \quad \theta_\alpha \quad \dot{\theta} \quad \dot{w}_\alpha \quad \dot{\theta}_\alpha]^T$  that is the angular, end-point residual and rotational displacements and velocities.  $\mathbf{0}_3$  is a  $3 \times 3$  null matrix,  $I_3$  is a  $3 \times 3$  identity matrix,  $\mathbf{0}_{3 \times 1}$  is a  $3 \times 1$  null vector and  $M_1^{-1}$  is the first column of  $M^{-1}$ . As the desired transfer function is from torque input to end-point residual output, the output matrix  $C$  is chosen as  $C = [0 \quad 1 \quad 0 \quad 0 \quad 0 \quad 0]$ .

With  $\alpha = \rho Al$  representing the weight and  $\beta = EI$  representing the flexural rigidity of the manipulator, the state-space matrices can be calculated. Thus, the system transfer function can be obtained as

$$G_1(s) = \frac{30\alpha^2 l^7 s^4 - 48600\alpha\beta l^4 s^2 + 4536000\beta^2 l}{s^2 [((15\alpha^2 l^8 + 3600\alpha l^6 I_h)M_p + \alpha^3 l^8 + 300\alpha^2 l^6 I_h)s^4 + ((39600\alpha\beta l^5 + 1512000\beta l^3 I_h)M_p + 5220\alpha^2 \beta l^5 + 367200\alpha\beta l^3 I_h)s^2 + (4536000\beta^2 l^2 M_p + 1512000\alpha\beta^2 l^2 + 4536000\beta^2 I_h)]} \quad (12)$$

Note that the transfer function is a closed form solution in terms of the system parameters.

## 4.0 ANALYSIS

In this section, the transfer function obtained in the previous section is analysed and assessed in the dynamic characterisation of the flexible manipulator system. This involves obtaining and investigating the system characteristics including poles, zeros, stability and vibration frequency. Relationships between the physical parameters and the system characteristics are then investigated. Note that in this work, the effect of damping is ignored. Therefore, the system is expected to be marginally stable, exhibiting a response of oscillatory nature.

### 4.1 System without Payload and Hub Inertia

For a flexible manipulator without payload and hub inertia, the system transfer function can be obtained by solving Eq. (12) with  $M_p = 0$  and  $I_h = 0$ . Thus, the transfer function from torque input to end-point residual can be obtained as

$$G(s) = \frac{30\alpha^2 l^7 s^4 - 48600\alpha\beta l^4 s^2 + 4536000\beta^2 l}{s^2(\alpha^3 l^8 s^4 + 5220\alpha^2\beta l^5 s^2 + 1512000\alpha\beta^2 l^2)} \quad (13)$$

Factoring the denominator and numerator polynomials of the transfer function yields system poles as

$$p = \pm j17.5444 \sqrt{\frac{\beta}{\alpha l^3}}, \quad \pm j70.087 \sqrt{\frac{\beta}{\alpha l^3}}, \quad 0, 0. \quad (14)$$

and the system zeros as

$$z = \pm 38.9944 \sqrt{\frac{\beta}{\alpha l^3}}, \quad \pm 9.9718 \sqrt{\frac{\beta}{\alpha l^3}} \quad (15)$$

Eqs. (14) and (15) demonstrate the relationship between system poles and zeros with the physical parameters of the manipulator. Thus the effects of each parameter on the system behaviour can be investigated. It is noted that all the poles lie on the imaginary axis of the s-plane whereas all the zeros lie on the real axis. Fig. 3 shows the effects of  $\beta$  on the system pole and zero. In this case, a constant  $\alpha = 0.15$  kg is considered. The result shows that the poles and zeros

move farther from the origin as  $\beta$  increases. Practically, changing the value of  $\beta$  implies changing the manipulator material.

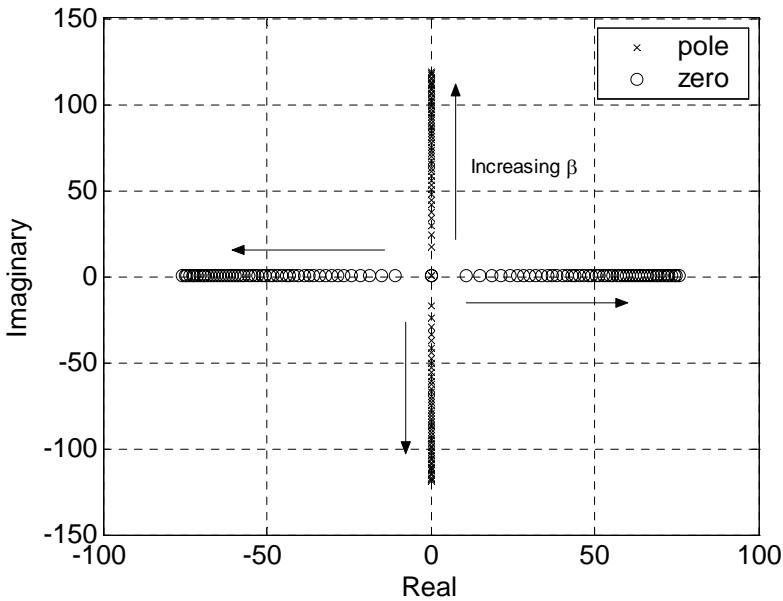


**Figure 3** Effects of flexural rigidity on the poles and zeros of the manipulator

The poles on the imaginary axis give the system natural frequencies. These, in turn, determine vibration modes of the system. Evaluating Eq. (14) yields vibration

$$\text{frequencies at modes 1 and 2 as } \frac{17.5444}{2\pi} \sqrt{\frac{\beta}{\alpha l^3}} \text{ Hz and } \frac{70.087}{2\pi} \sqrt{\frac{\beta}{\alpha l^3}} \text{ Hz}$$

respectively. Fig. 4 shows the effect of flexural rigidity,  $\beta$  of a manipulator on the vibration frequencies of modes 1 and 2 with a constant weight of the manipulator. Similarly, the inter-relation between  $\alpha$  and the poles, zeros and vibration frequencies of the system with a constant flexural rigidity can be investigated. The result with  $\beta = 3.69 \text{ Nm}^2$  is shown in Fig. 5. It is also important to investigate, for the same material, the effect of changing the manipulator length on vibration frequency. Fig. 6 shows the result with two different materials,  $\beta = 1.2 \text{ Nm}^2$  and  $3.6 \text{ Nm}^2$ . The results show that the poles/vibration frequencies reduce as the manipulator length increases. However, for the different materials, as length increases, the differences of the poles/vibration frequencies become insignificant.

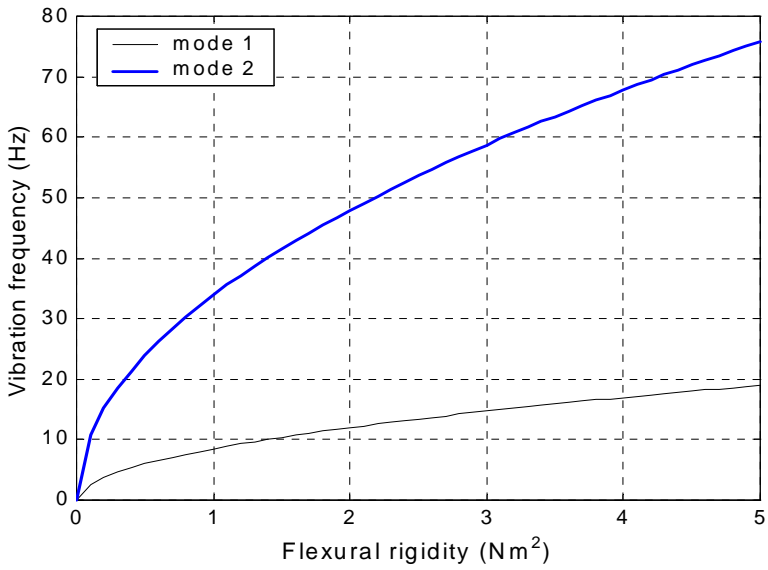


**Figure 4** Effect of flexural rigidity on vibration frequency ( $\alpha = 0.15$  kg)

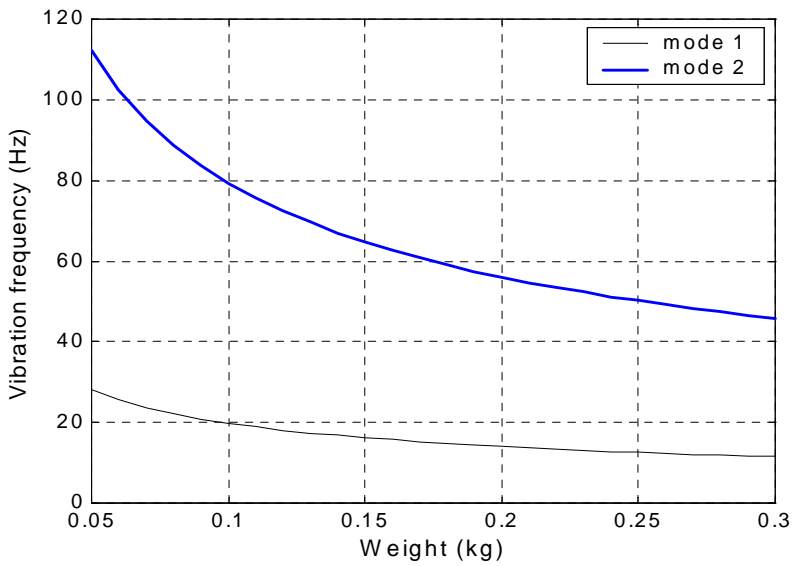


**Figure 5** Effect of the weight of a manipulator on vibration frequency ( $\beta = 3.69$  Nm<sup>3</sup>)

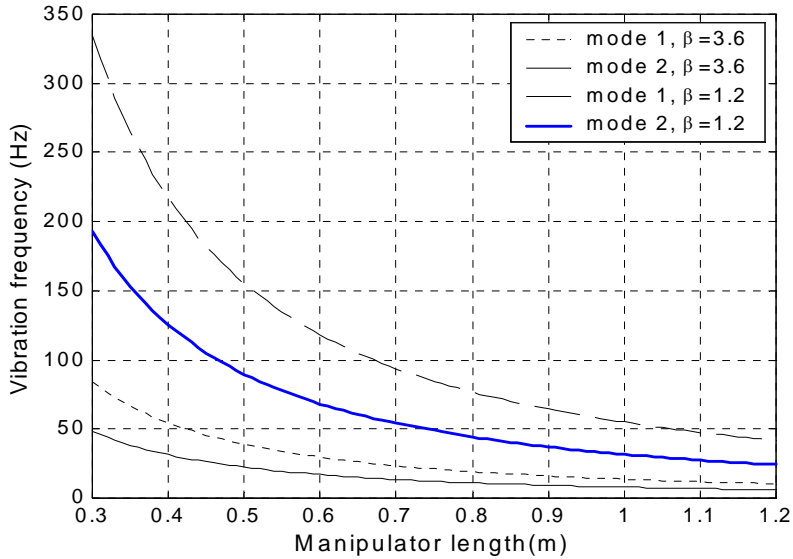


**Figure 6** Effect of length of a manipulator on vibration frequency with two types of material

The zeros will determine whether the system exhibits minimum-phase or non-minimum phase behaviour and will determine the magnitude of response of the system. It is noted from Eq. (15) that, with any values of  $\alpha$ ,  $\beta$  and  $l$ , two zeros lie on the right half of s-plane (rhp) and the others on the left half of s-plane (lhp). Thus, the system is non-minimum phase and undershoot is expected at the start in the end-point residual response. This agrees, with the result reported earlier in respect of a system incorporating non-collocated sensors and actuators. By obtaining the relationships between poles, zeros and vibration frequencies with the physical parameters of the manipulator, the dynamic behaviour of an actual system could be predicted prior to the actual design. Moreover, in design, important information that can be used to achieve several objectives is available.

## 4.2 System with Payload

It is noted from the transfer function in Eq. (12) that the payload term is not in the numerator of the transfer function. Therefore, payload does not affect the system zeros and the behaviour of the system zero is similar as the case without payload. Furthermore, it is noted that the flexible manipulator is a type two system, which implies that zero steady-state error can only be achieved using step and ramp command inputs to the system.

The system poles, on the other hand, are affected by the payload, see Eq. (12). To investigate the effects of payload on the dynamic behaviour of the system, the transfer function was solved with a system constituting an aluminium type flexible arm of dimensions  $900 \times 3.2004 \times 19.008$  mm,  $E = 71 \times 10^9$  N/m<sup>2</sup>,  $I = 5.1924 \times 10^{-11}$  m<sup>4</sup>,  $\rho = 2710$  kg/m<sup>3</sup> and  $I_h = 5.8598 \times 10^{-4}$  kgm<sup>2</sup>. These parameters correspond to a physical flexible manipulator experimental rig designed for experimental verification of modelling and controller designs involving flexible manipulators [2]. Thus, the denominator of the system transfer function can be obtained as

$$(0.3M_p + 0.0035)s^6 + (15370.2M_p + 340.36)s^4 + (5.13 \times 10^7 M_p + 2571860)s^2 \quad (16)$$

Therefore, the poles in terms of payload can be obtained as

$$p_{1,2} = \pm 6.09 \sqrt{\frac{6.47h - (351.5M_p + 7.8)}{0.5M_p + 0.006}}, \quad (17)$$

$$p_{3,4} = \pm 6.09 \sqrt{\frac{-6.47h - (351.5M_p + 7.8)}{0.5M_p + 0.006}}, \quad p_5 = 0, \quad p_6 = 0$$

where  $h = \sqrt{2161.6M_p^2 + 82.2M_p + 1.0}$ .

Note that for a single element, the system has six poles, two of which are at the origin. Since for  $M_p \geq 0$ , the terms under the square roots in Equation (17) are negative, the remaining poles are purely imaginary and lie on the imaginary axis of the s-plane. These result, as expected for a system without damping, a marginally stable system. The system poles give the system vibration frequencies. Thus, the effects of payload on the vibration frequency can also be investigated by solving Equation (17). Figure 7 demonstrates the relationship between payload and system vibration frequencies for modes 1 and 2. It is noted that with increasing payload, the vibration frequencies decrease significantly.

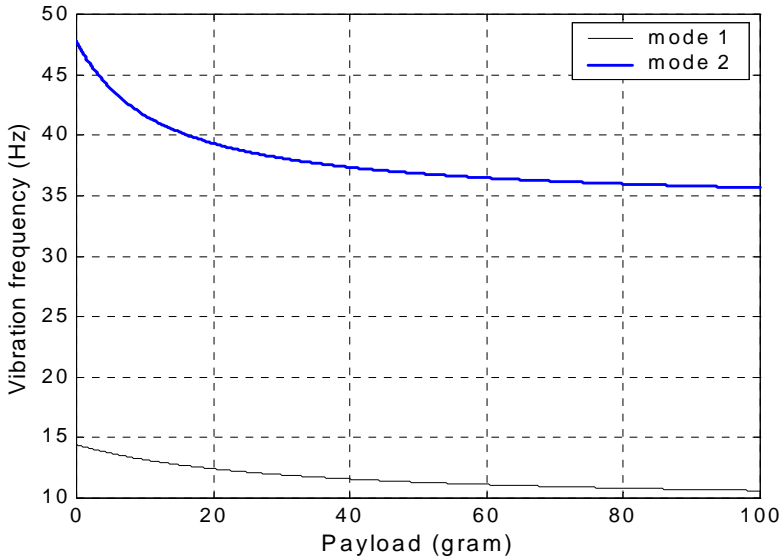


**Figure 7** Effect of payload on the vibration frequency of the system

Since control of a non-minimum phase system is rather involved, this aspect is further analysed in this section. For the transfer function from the torque input to end-point residual that exhibits a non-minimum phase characteristic, it is important to investigate whether the zeros can be relocated to the lhp by altering physical parameters of the system. If so, in designing an actual flexible manipulator, certain parameter values can be considered to make the system minimum phase. In this work, the analyses are carried out using the Routh-Hurtwitz (RH) criterion. Accordingly, if there is no sign change in the first column of RH table, then all roots of the polynomial will be on the lhp. Utilising the RH criterion, the first column of RH table for numerator of transfer function is shown in Table 1. It is noted that there are two sign changes, that are from  $s^3$  to  $s^2$  and  $s^1$  to  $s^0$ , indicating that two zeros exist on the rhp. It can be concluded that, since all terms are single, the zeros cannot be relocated by altering any physical parameter value.

## 5.0 VIBRATION CONTROL SCHEME

This section presents a case study where symbolic algebra is used for the development of an effective vibration control algorithm for a flexible manipulator.

**Table 1** The first column of RH table for the numerator of the transfer function

$s^4$	$30\alpha^2 l^7$
$s^3$	$120\alpha^2 l^7$
$s^2$	$-24300\alpha\beta l^4$
$s^1$	$-74800\alpha\beta l^4$
$s^0$	$4536000\beta^2 l$

In this work, the symbolic results obtained in the previous section are utilised to design an input shaping control algorithm. Simulation results are presented to demonstrate the application of symbolic algebra in controller design and the performance of the controller in suppressing the system vibration.

Input shaping technique is a feedforward control and a practical technique to suppress vibration of flexible structures. Previous experimental exercises have shown that the method is effective in suppressing vibration of flexible manipulators [10]. The method involves convolving a desired command with a sequence of impulses known as input shaper. This yields a shaped input that drives the system to a desired location with reduced vibration. The input shaping process is illustrated in Fig. 8 where  $A_i$  and  $t_i$  are the magnitudes and time locations at which the impulses occur. Design objectives are to determine the amplitude and time locations of the impulses, based on the vibration frequencies and damping ratios of the system.



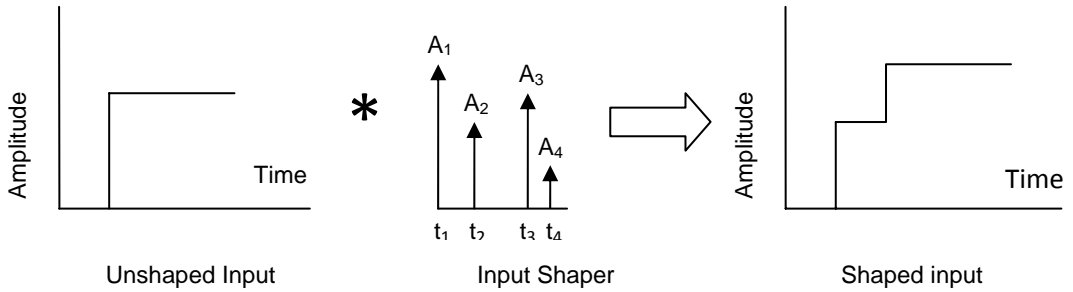


**Figure 8** Illustration of input shaping technique

Utilising the input shaping technique, to achieve zero vibration and higher robustness for a single vibration mode, an input shaper with a four-impulse sequence can be designed with parameters as

$$t_1 = 0, \quad t_2 = \frac{\pi}{\omega_n \sqrt{1-\zeta^2}}, \quad t_3 = 2t_2, \quad t_4 = 3t_2 \tag{18}$$

$$A_1 = \frac{1}{1+3K+3K^2+K^3}, \quad A_2 = \frac{3K}{1+3K+3K^2+K^3}, \tag{19}$$

$$A_3 = \frac{3K^2}{1+3K+3K^2+K^3}, \quad A_4 = \frac{K^3}{1+3K+3K^2+K^3}.$$

where  $K = e^{-\frac{\zeta\pi}{\sqrt{1-\zeta^2}}}$ ,  $\omega_n$  is the natural frequency and  $\zeta$  is the damping ratio of the system. To handle other vibration modes, an input shaper for each vibration mode can be designed independently. Then the impulse sequences can be convoluted together to form a sequence of impulses that attenuate vibration at required modes.

However, as the vibration frequencies of the system is significantly affected by payload variations, locations of the impulses have to be re-calculated to achieve a similar level of vibration reduction. In this case, a closed form solution that provides the relationship between payload, vibration frequencies and impulse locations can be utilised to automate the process of updating the input shaper. Fig. 9 shows a block diagram of the input shaping vibration control scheme where the input shaper is updated according to the payload of the manipulator based on the symbolic model. The locations of the impulses in terms of payload can be obtained by substituting Eqs. (17) into (18). This yields the location of the second impulse for mode 1 as

$$t_2 = \left[ 12.18 \sqrt{\frac{(6.47h - (351.5M_p + 7.8))(1 - \zeta^2)}{0.5M_p + 0.006}} \right]^{-1} \tag{20}$$

and mode 2 as

$$t_2 = \left[ 12.18 \sqrt{\frac{(-6.47h - (351.5M_p + 7.8))(1 - \zeta^2)}{0.5M_p + 0.006}} \right]^{-1} \tag{21}$$

where  $h$  as in Eq. (17). The other impulse locations can be determined based on the second impulse as shown in Eq. (18).

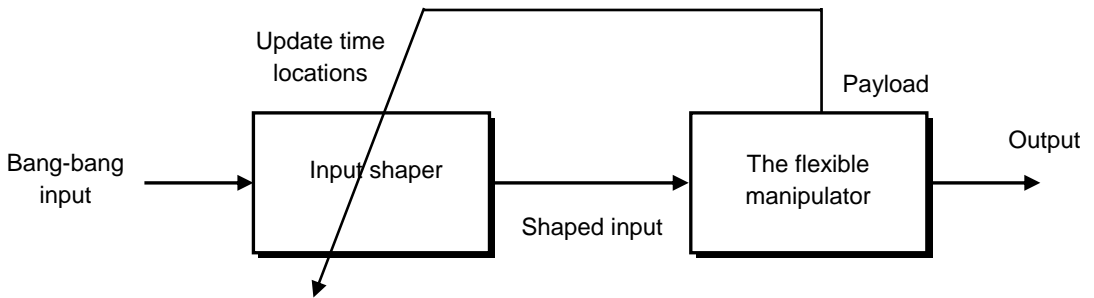


**Figure 9** Block diagram of the input shaping control based on payload of the flexible manipulator

To demonstrate the performance of the controller in suppressing the system vibration, simulated exercises are given in this section. To allow this, the system parameters given in Section 3 are considered. In these exercises, a single switch bang-bang input of amplitude 0.3 Nm shown in Fig. 10 is used as input torque and applied at the hub of the manipulator. Fig. 11 shows the end-point residual response of the manipulator without payload and with 50 grams payload to the input torque. This is obtained by multiplying the system transfer function with the input torque and utilising the inverse Laplace transform. The results demonstrate that significant vibrations occur at the end-point during the movement of the manipulator.

In order to design the input shaper for control of vibration, the amplitudes and locations for the impulses have to be determined. Previous experimental results on the flexible manipulator have shown that the damping ratios of the system are 0.026 and 0.038 for the first two modes of vibration [2]. Thus, the impulse magnitudes can be determined by solving Eq. (19). Moreover, for a particular system, the damping ratios are normally constants. For the impulse locations, the solutions in Eqs. (20) and (21) can be utilised to automate the calculation of the impulse locations based on payload to achieve a similar level of vibration reduction. By solving Eqs. (20) and (21) for the system without payload,  $t_2$  is obtained as 0.0357 sec and 0.0106 sec for mode 1 and 2 respectively. Similarly, with 50 grams payload,  $t_2$  is obtained as 0.0434 sec and 0.014 sec.

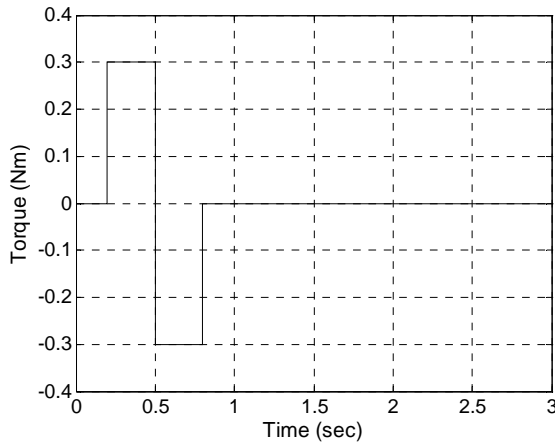


**Figure 10** The bang-bang input torque

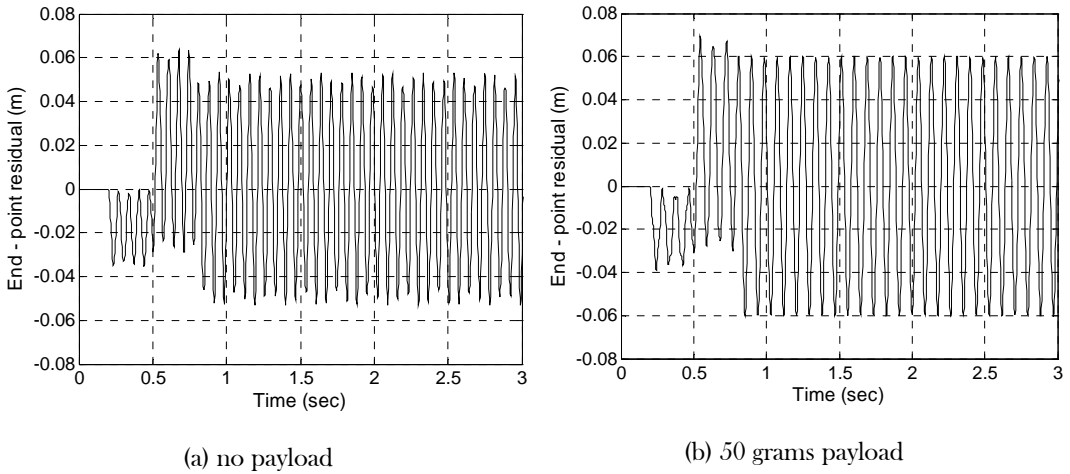


**Figure 11** End-point residual response of the flexible manipulator without input shaping control

Fig. 12 show the end-point residual responses of the system without payload and 50 grams payload to the shaped inputs. It is noted that the system vibrations have significantly been reduced as compared to the response without input shaper (Fig. 11). Further investigations show that vibration reductions of 24 dB were achieved in both cases. This demonstrates the advantage of using symbolic algebra in designing an effective vibration control algorithm for flexible manipulators with varying payloads.

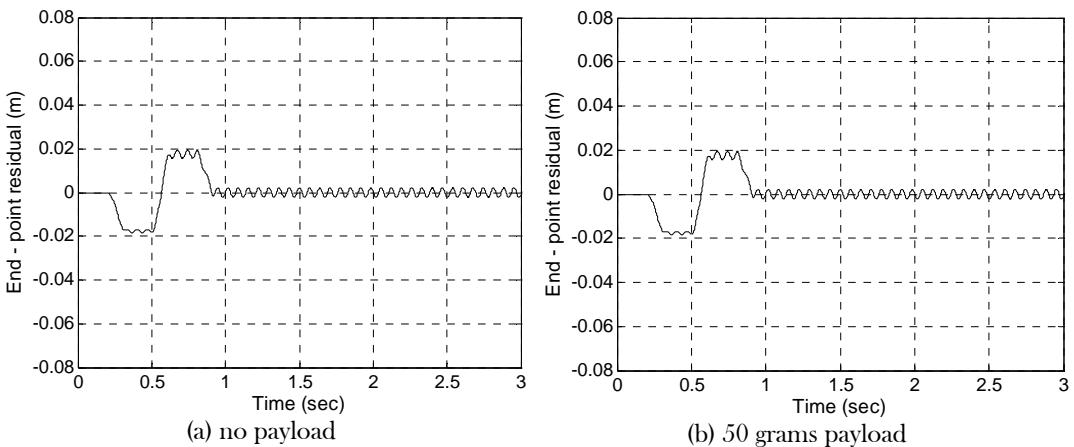


**Figure 12** End-point residual response of the flexible manipulator with input shaping control

## 6.0 CONCLUSIONS

The application of computer algebra for modelling and vibration control of a flexible manipulator system has been presented. It has been demonstrated that the symbolic approach provides several advantages in characterising the dynamic behaviour of the manipulator, in assessing the stability, response and vibration frequency of the system and designing an effective vibration control algorithm. The system transfer function has been obtained in symbolic form and thus interrelations between physical parameters including payload of the manipulator and system characteristics have been investigated. The symbolic approach has also been utilised to develop an input shaping control algorithm to control a flexible manipulator with varying payloads. Simulation results have been presented demonstrating the performance of the symbolic approach in modelling and control of the flexible manipulator system. It can be concluded that the symbolic-based results are very helpful in understanding the dynamic behaviour and controller design of a flexible manipulator.

## REFERENCES

- [1] Tokhi, M.O., Z. Mohamed, and M.H. Shaheed. 2001. Dynamic Characterisation of a Flexible Manipulator System. *Robotica*. 19: 571-580.
- [2] Martins, J. M., Z. Mohamed, M. O. Tokhi, J. Sá da Costa, and M.A. Botto. 2003. Approaches for Dynamic Modelling of Flexible Manipulator Systems. *IEE Proceedings-Control Theory and Application*. 150: 401-411.
- [3] Aoustin, Y., C. Chevallereau, A. Glumineau, and C. H. Moog. 1994. Experimental Results for the End-Effector Control of a Single Flexible Robotic Arm. *IEEE Transactions on Control Systems Technology*. 2: 371-381.
- [4] Larcombe, P. J., and I. C. Brown. 1997. Computer Algebra: A Brief Overview and Application to Dynamic Modelling. *Journal of Computing and Control Engineering*. 8: 53-57.
- [5] Cetinkunt, S., and B. Itop. 1992. Computer-automated Symbolic Modeling of Dynamics of Robotic Manipulators with Flexible Links. *IEEE Transactions of Robotics and Automation*. 8: 94-105.
- [6] Lin, J., and F. L. Lewis. 1994. A Symbolic Formulation of Dynamic Equations for a Manipulator with Rigid and Flexible Links. *International Journal of Robotics Research*. 13: 454-466.
- [7] Pota, H. R., and T. E. Alberts. 1995. Multivariable Transfer Functions for a Slewing Piezoelectric Laminate Beam. *Transactions of the ASME Journal of Dynamic Systems, Measurement, and Control*. 117:352-359.
- [8] Low, K. H., and M. Vidyasagar. 1988. A Lagrangian Formulation of Dynamic Model for Flexible Manipulator Systems. *Transactions of ASME: Journal of Dynamic Systems, Measurement and Control*. 110:175-181.
- [9] Tzes, A. P., S.Yurkovich, and F. D. Langer. 1989. A Method for Solution of the Euler-Bernoulli Beam Equation in Flexible-link Robotic Systems. *Proceedings of IEEE International Conference on Robotics and Automation*. Scottsdale. 557-560.
- [10] Mohamed, Z., J. M. Martins, M. O. Tokhi, J. Sá da Costa, and M. A. Botto. 2005. Vibration Control of a Very Flexible Manipulator System. *Control Engineering Practice*. 13: 267-277.